JPE 5-2-8

Diminution of Current Measurement Error in Vector Controlled AC Motor Drives

Han-Su Jung*, Jang-Mok Kim†, Cheul-U Kim*, Cheol Choi**, and Tae-Uk Jung***

†*Dept. of Electrical Engineering, Pusan National University, Busan, Korea
**Servo R&D Part, OTIS-LG
***Digital Appliance Company, LG Electronics Inc.

ABSTRACT

The errors generated from current measurement paths are inevitable, and they can be divided into two categories: offset error and scaling error. The current data including these errors cause periodic speed ripples which are one and two times the stator electrical frequency respectively. Since these undesirable ripples bring about harmful influences to motor driving systems, a compensation algorithm must be introduced to the control algorithm of the motor drive. In this paper, a new compensation algorithm is proposed. The signal of the integrator output of the d-axis current regulator is chosen and processed to compensate for the current measurement errors. Usually the d-axis current command is zero or constant to acquire the maximum torque or unity power factor in the ac drive system, and the output of the d-axis current regulator is nearly zero or constant as well. If the stator currents include the offset and scaling errors, the respective motor speed produces a ripple related to one and two times the stator electrical frequency, and the signal of the integrator output of the d-axis current regulator also produces the ripple as the motor speed does. The compensation of the current measurement errors is easily implemented to smooth the signal of the integrator output of the d-axis current regulator by subtracting the DC offset value or rescaling the gain of the hall sensor. Therefore, the proposed algorithm has several features: the robustness in the variation of the mechanical parameters, the application of the steady and transient state, the ease of implementation, and less computation time. The MATLAB simulation and experimental results are shown in order to verify the validity of the proposed current compensating algorithm.

Keywords: current measurement error, speed ripple, torque ripple, offset error, scaling error

1. Introduction

Recently, vector control has become essential in operating an ac motor. In the vector control, a precise current measurement is very important[1-2]. Stator currents are measured through hall sensors, low pass filters and A/D converters. Because of the non-linearity of the hall sensor, thermal drift of analog elements, and the quantization errors of the A/D converters, the errors generated from current paths are inevitable even if the system shows consistency and a high degree of maintenance.

Fig.1 summarizes the types of errors in the digital ac motor drive system[3]. These types of errors will appear as

---

Manuscript received December 22, 2004; revised March 7, 2005

†Corresponding Author: jmok@pusan.ac.kr, Pusan National Univ. Tel: +82-51-510-2366, Fax: +82-51-510-0212
*Dept. of Electrical Eng., Pusan National Univ.
**Servo R&D Part, OTIS-LG

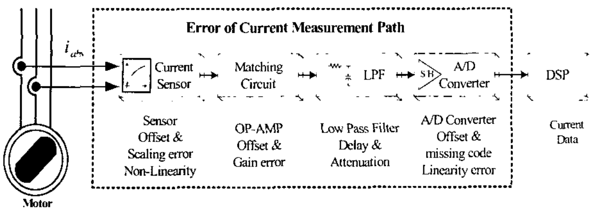

Fig. 1 Error path of current measurement

offset and scaling errors in the end.

When the stator currents include the offset and scaling errors, torque pulsation occurs corresponding to one and two times of stator electrical frequency respectively. This results in the deterioration of the performance of the motor drive system. Specifically, this influence must be considered for the control of the ultra precision position [4] and a compensation method is added in the control algorithm of the motor drive.

When the stator currents include the offset and scaling errors, torque pulsation occurs corresponding to one and two times of stator electrical frequency respectively. This results in the deterioration of the performance of the motor drive system. Especially, influence of those must be considered for the control of the ultra precision position [4] and a compensation method is to be added in the control algorithm of the motor drive.

The recent studies have reported that the undesirable periodic ripple element was related by the error in current measurement. One in [5] and [6] utilizes the inverse system model to calculate the torque ripple. So this method may become unstable with inexact mechanical parameters. Another in [7] and [8] requires a torque sensor, and this may be unacceptable in many application fields. The other in [9] is robust in the variations of the mechanical parameters and can be applied to wide speed ranges. It is, however, difficult to implement this compensation algorithm in real systems. All methods mentioned above can only be applied to the steady state operation.

In this paper a new compensation method is proposed. The main contribution of this paper introduces the signal of the integrator output of the d-axis current regulator to compensate for the errors of the current measurement. Usually the d-axis current command is zero or constant to acquire the maximum torque or unity power factor in the ac drive system, and the output of the d-axis current regulator is nearly zero or constant as well. If the stator currents include the offset and scaling errors, the motor speed has the ripple related to one and two times of the stator electrical frequency respectively, and the signal of the integrator output of the d-axis current regulator also has the ripple as the motor speed does. The compensation of the current measurement errors is easily implemented to smooth the signal of the integrator output of the d-axis current regulator by subtracting the DC offset value or rescaling the gain of the hall sensor.

2. The Effect of Current Measurement Error

2.1 Effect of offset error

The offset error, which may be caused by a potential imbalance of a sensor device, measurement path, or some other unforeseen factor is inevitable. It is common that the offset current is calculated by reading A/D converter repeatedly without current flowing. But the effects of the thermal drift of analog devices and the switching noise in the actual running condition are not considered in this case.

The error of offset can be expressed in an actual 3 phase system by (1).

$$\begin{aligned} I_{as\_sens} &= I_{as} + \Delta I_{as} \\ I_{bs\_sens} &= I_{bs} + \Delta I_{bs} \\ I_{cs\_sens} &= -\left(I_{as\_sens} + I_{bs\_sens}\right) \end{aligned} \tag{1}$$

Since the summation of the three phases current values should be zero in case there is no neutral point inter-connection, it is sufficient to measure only two phase currents for the vector control. From (1) the measured synchronous d-q axis currents can be calculated as follows:

$$\begin{aligned} I^e_{ds\_sens} &= I^e_{ds} + \Delta I^e_{ds} \\ I^e_{qs\_sens} &= I^e_{qs} + \Delta I^e_{qs} \end{aligned} \tag{2}$$

where

$$\Delta I^e_{ds} = \Delta I_{as} \cos\theta_e + \frac{1}{\sqrt{3}}\left(2\Delta I_{bs} + \Delta I_{as}\right)\sin\theta_e \tag{3}$$

$$\Delta I^e_{qs} = -\Delta I_{as} \sin\theta_e + \frac{1}{\sqrt{3}}\left(2\Delta I_{bs} + \Delta I_{as}\right)\cos\theta_e \tag{4}$$

ΔI^e_{ds} and ΔI^e_{qs} contain the ripple corresponding to the undamental value of the stator electrical frequency.

2.2 Effect of Scaling error

The scaling error may be caused by non-linearity of the current sensor itself, the matching circuit between the current sensor and A/D input, the quantization errors and non-linearity of an A/D converter [10].

Usually the d-axis current command is zero or constant to obtain maximum torque in a constant torque region. If the stator currents contain the scaling error, the stator currents can be expressed as (5). Where K_a and K_b denote the scale factor of *a*, *b* phase current respectively. The minus sign merely reflects the reference angle of *a-b* phases.

$$\begin{aligned} I_{as\ \ sens} &= -K_a I\,sin\,\theta_e \\ I_{bs\ \ sens} &= -K_b I\,sin\left(\theta_e - \frac{2}{3}\pi\right) \end{aligned} \tag{5}$$

From (5) the measured synchronous *d-q* axis currents can be acquired as follows:

$$\begin{aligned} \Delta I^e_{ds\_scale} &= I^e_{ds\ \ sens} - I^e_{ds} \\ &= \frac{(K_b - K_a)}{\sqrt{3}} I \sin\left(2\theta_e + \frac{\pi}{6}\right) + \frac{(K_a - K_b)}{2\sqrt{3}} I \end{aligned} \tag{6}$$

$$\begin{aligned} \Delta I^e_{qs\ \ scale} &= I^e_{qs\ \ sens} - I^e_{qs} \\ &= \frac{(K_b - K_a)}{\sqrt{3}} I \sin\left(2\theta_e + \frac{1}{3}\pi\right) + \frac{(K_a + K_b)}{2} I \end{aligned} \tag{7}$$

As known from $\Delta I^e_{ds\_scale}$ and $\Delta I^e_{qs\_scale}$, *d-q* axis currents contain the ripple corresponding to two times ($2f_e$) of the stator electrical frequency.

3. The Compensation Method for Current Measurement Error

3.1 Analyzing the signal of the integrator output of the d-axis current regulator

If the stator currents include the offset and scaling errors, the signal of the integrator output of the d-axis current regulator also has the ripple related to one and two times of the stator electrical frequency respectively as mentioned above. This signal can be derived by integrating the sum of (3) and (6) as follows in (8):

$$K_i \int_0^t (i^{e*}_{ds} - i^e_{ds\_sens})dt = -K_i \int_0^t \Delta i^e_{ds}\,dt \tag{8}$$

As known from (3) and (6), (8) contains the ripple corresponding to one, two and six times of the stator electrical frequency respectively. Six times frequency ripple reflects the effect of the dead time of the switching device[11-14]. In order to remove or ignore the dead time effect, it is necessary to average (8) between the interval [0 2π] as shown in Fig. 2. To get the average value, splitting the interval [0 2π] into 6 parts as shown in Fig.2, and integrating 6 parts result in the elimination of the dead time effect by averaging 6 parts respectively.

3.2 Proposed Compensation Method

3.2.1 Offset errors Compensation

Fig. 2 shows the results of two cases. One case is dividing (8) into two segments (secA and secB) and integrating as known in Fig. 2(a). And the result of calculation of secA and secB is shown in (9) and (10) respectively.

$$\sec A = \int_0^{\pi} \int_0^t -K_i \Delta I^e_{ds} dt\ d\theta_e = -2\frac{K_i}{\omega_e}\Delta I_{as} \tag{9}$$

$$\sec B = \int_{\pi}^{2\pi} \int_0^t -K_i \Delta I^e_{ds} dt\ d\theta_e = 2\frac{K_i}{\omega_e}\Delta I_{as} \tag{10}$$

The difference (ε_1) reflects the existence of a-phase offset error (ΔI_{as}), and is (11) as follows:

$$\varepsilon_1 = sec1 - sec2 = -4\frac{K_i}{\omega_e}\Delta I_{as} \tag{11}$$

This error (ε_1) is easily removed or compensated by equalizing the integral values between two segments. The other case is dividing (8) into six segments (sec Ⅰ ~ secⅥ) and integrating as shown in Fig. 2(b) and (c).

Nevertheless the signal of the integral output of d-axis current regulator has the offset error, sec Ⅰ, secⅢ, sec Ⅳ and secVI have the different values as shown in Fig. 2(b), and (12).

$$
\begin{aligned}
\sec I &= \int_0^{\frac{\pi}{3}} \int_0^t -K_i \Delta I_{ds}^e dt\ d\theta_e = \frac{K_i}{\omega_e} \Delta I_{bs} \\
\sec III &= \int_{\frac{2\pi}{3}}^{\pi} \int_0^t -K_i \Delta I_{ds}^e dt\ d\theta_e = \frac{K_i}{\omega_e} (\Delta I_{as} - \Delta I_{bs}) \\
\sec IV &= \int_{\pi}^{\frac{4\pi}{3}} \int_0^t -K_i \Delta I_{ds}^e dt\ d\theta_e = -\frac{K_i}{\omega_e} \Delta I_{bs} \\
\sec VI &= \int_{\frac{5\pi}{3}}^{2\pi} \int_0^t -K_i \Delta I_{ds}^e dt\ d\theta_e = \frac{K_i}{\omega_e} (\Delta I_{as} + \Delta I_{bs})
\end{aligned} \tag{12}
$$

The summation (ε_2) between ε_a and ε_b explains the existence of b-phase offset error (ΔI_{bs}) as shown in Fig.2 (b), and (13).

$$
\begin{aligned}
\varepsilon_a &= \sec IV - \sec I, \\
\varepsilon_b &= \sec III - \sec VI \\
\varepsilon_2 &= \varepsilon_a + \varepsilon_b = -4\frac{K_i}{\omega_e} \Delta I_{bs}
\end{aligned} \tag{13}
$$

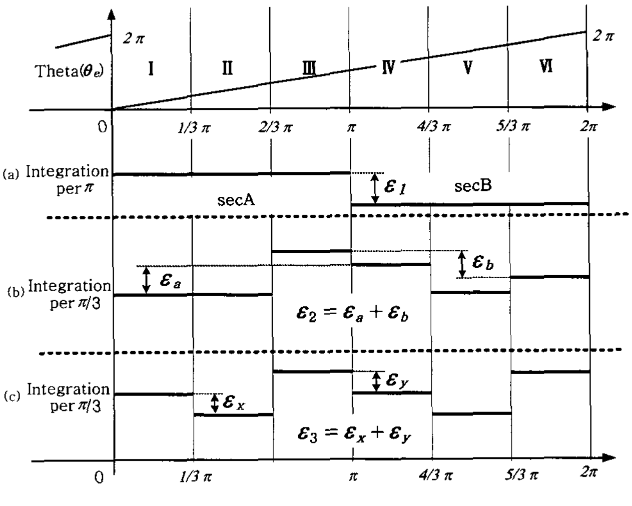

Fig. 2 Each error(ε_1,ε_2,ε_3)of current analyzed for compensation

If offset errors (ε_1 and ε_2) are completely compensated or removed, each segment shows values as (14) respectively. (14) is always satisfied although scaling errors are in the signal of the integrator output of the d-axis current regulator.

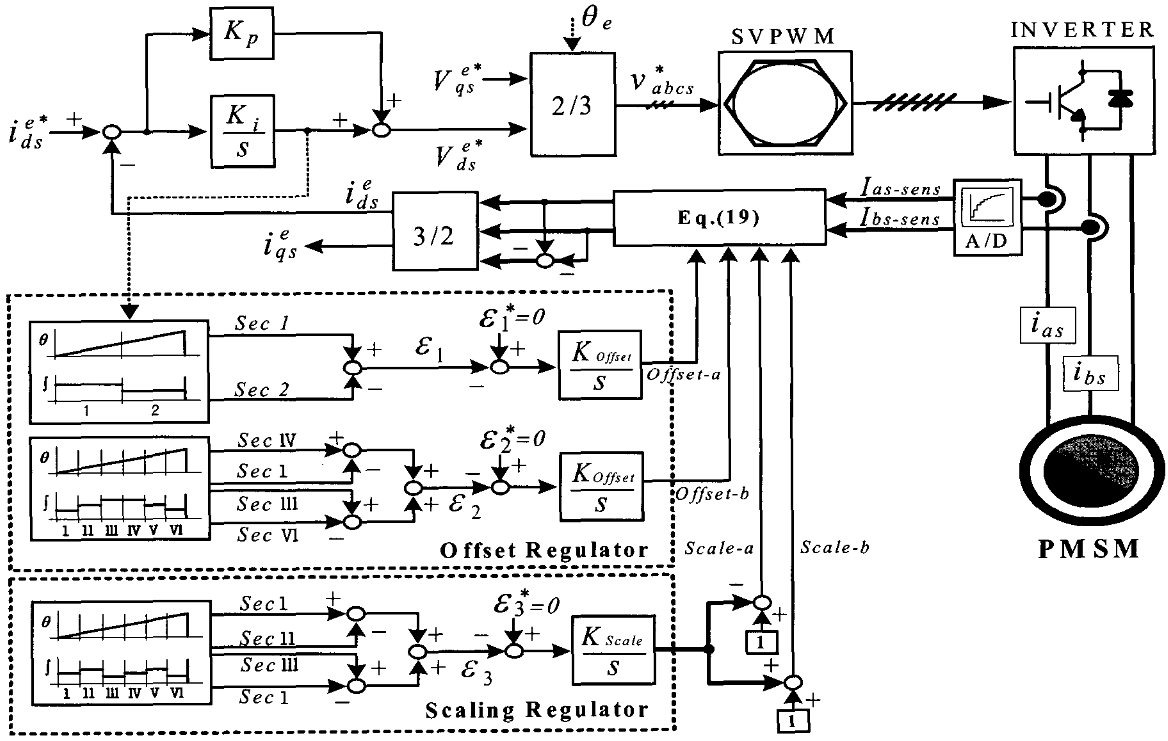

Fig. 3 Main block diagram of the proposed compensation scheme.

$$\begin{aligned} sec\,I &= sec\,IV, \\ sec\,II &= sec\,V, \\ sec\,III &= sec\,VI \end{aligned} \tag{14}$$

3.2.2 Scaling Errors Compensation.

If the scaling factors (K_a and K_b) of a- and b-phase have the same value, (6) and (7) are zero and not observed. In this case the compensation of the scaling effect is completed. (15), (16) and (17) reflect the existence of scaling errors.

$$sec\,I = \int_0^{\frac{\pi}{3}} \int_0^t -K_i \Delta I^e_{ds-scale} dt\, d\theta_e = 0 \tag{15}$$

$$\mathrm{sec}II = \int_{\frac{\pi}{3}}^{\frac{2\pi}{3}} \int_0^t -K_i \Delta I^e_{ds-scale} dt\, d\theta_e = -\frac{3K_i(K_b - K_a)I}{8\sqrt{3}\omega_e} \tag{16}$$

$$\mathrm{sec}III = \int_{\frac{2\pi}{3}}^{\pi} \int_0^t -K_i \Delta I^e_{ds-scale} dt\, d\theta_e = \frac{3K_i(K_b - K_a)I}{8\sqrt{3}\omega_e} \tag{17}$$

The summation (ε_3) between ε_x and ε_y explains the existence of scaling errors between a- and b-phase as shown in Fig.2 (c), and (18).

$$\begin{aligned} \varepsilon_x &= \sec I - \sec II, \\ \varepsilon_y &= \sec III - \sec IV \\ \varepsilon_3 &= \varepsilon_x + \varepsilon_y = \frac{\sqrt{3}K_i(K_b - K_a)}{4\omega_e} \end{aligned} \tag{18}$$

Scaling error (ε_3) is easily removed or compensated by making ε_3 null or zero. Both scaling factors have approximate unity ($K_a \cong 1$, and $K_b \cong 1$), compensation is carried out about two phases simultaneously until $\varepsilon_3 = 0$.

3.2.3 Implementation of the Proposed Compensation Algorithm

Fig.3 shows the main conceptual block diagram of the proposed compensation method. The signal of the integrator output of d-axis current regulator is used to the input of the proposed compensation algorithm. This algorithm consists of offset and scaling parts. The integral outputs of the offset part are (11) and (13). These terms are the input of the I-type (Integral-type) controller(K_{offset}/S). The two I-type controllers of the offset part force ε_1 and ε_2 to be zero. The integral outputs of the scaling part are (18). This term is the input of the I-type controller (K_{scale}/S). Also the I-type of the scaling part forces ε_3 to be zero. The I-type controller includes a function of the memory which stores compensation value at this point. The compensation of offset and scaling errors is achieved automatically in the proposed compensation algorithm and the compensation direction corresponds to table 1. The compensating gains (K_{offset} and K_{scale}) of the offset and scaling errors can be chosen between 0 and 1. The smaller gain, the slower response, but more accurate compensation current can be achieved. In this paper, $K_{offset} = 0.1$ and $K_{scale} = 0.05$ are chosen for stable operation. The compensation gains of offset and scaling errors are obtained by multiplying ω_e by K_{offset} and K_{scale}, and the same accuracy of the compensation is guaranteed according to the rotor speed. The compensating action is finally achieved by (19) from output (*Offset-a, Offset-b, Scale-a, Scale-b*) of the I-type controller.

$$\begin{aligned} I_{as} &= I_{as-sens} \times S_{cale-a} - O_{ffset-a} \\ I_{bs} &= I_{bs-sens} \times S_{cale-b} - O_{ffset-b} \end{aligned} \tag{19}$$

The compensation direction of the proposed algorithm is summarized in Table 1.

Table 1 Compensation directions to adjust the offset and scaling errors

Value	Error of Integral Value	Error of measured Current	Direction of Compensation
Offset-a	$\varepsilon_1 > 0$	$\Delta I_{as} < 0$	(+)
	$\varepsilon_1 < 0$	$\Delta I_{as} > 0$	(−)
Offset-b	$\varepsilon_2 > 0$	$\Delta I_{bs} < 0$	(+)
	$\varepsilon_2 < 0$	$\Delta I_{bs} > 0$	(−)
Scale-a	$\varepsilon_3 > 0$	$K_a < K_b$	(+)
	$\varepsilon_3 < 0$	$K_a > K_b$	(−)
Scale-b	$\varepsilon_3 > 0$	$K_a < K_b$	(−)
	$\varepsilon_3 < 0$	$K_a > K_b$	(+)

4. Simulation

The simulation of the proposed algorithm was performed by using MATLAB Simulink[15]. To verify the feasibility and effectiveness of the proposed compensation algorithm, the current errors of offset and scaling are given, $\Delta I_{as}=0.05[A]$, $\Delta I_{bs}=0.02[A]$, $K_a=1.1$ and $K_b=0.9$ respectively in this simulation. Fig.4 is simulation block in order to verify the validity of the proposed compensating algorithm. In the upper parts are the speed controller for a motor, a current controller and a modeled motor. In the lower parts are the path of current measurement and compensator for the verification of algorithm. Fig. 2 shows simulation block of the proposed compensation scheme.

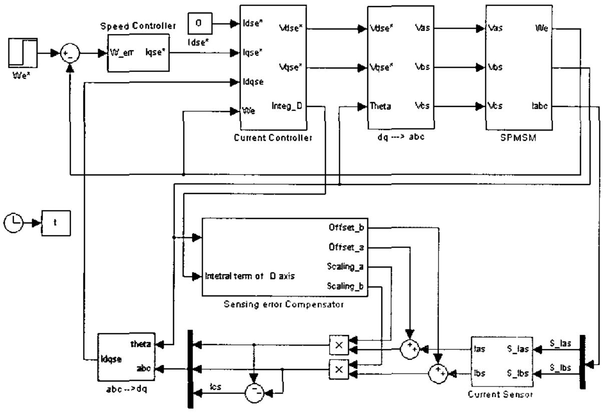

Fig. 4 Simulation block of the proposed compensation scheme

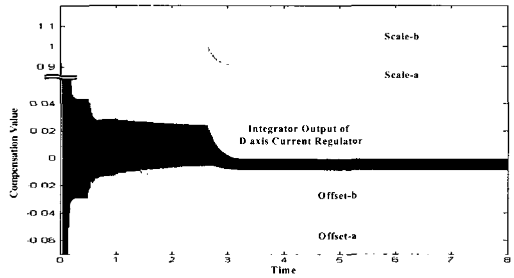

(a) Ripple reduction with the proposed compensation scheme

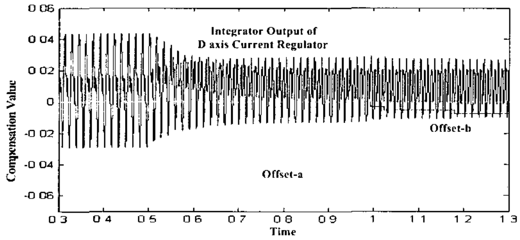

(b) Extension of (a) between 0.3[sec] and 1.3[sec]

Fig. 5 Simulation results

Fig. 5 shows the simulation waveforms of the integrator output of the d-axis current regulator, and the starting time of the compensation is at 0.5[sec]. The compensation operation of offset and scaling are carrying out at the same time as shown in Fig. 5(a). And Fig. 5(b) is a larger scale of Fig. 5(a). These waveforms show that the proposed algorithm operates well under these conditions.

5. Experimental Results

Fig. 6 shows the AC motor drive system used in the experiment. In this experiment, 50,000pps encoder is used for the precise speed measurement.

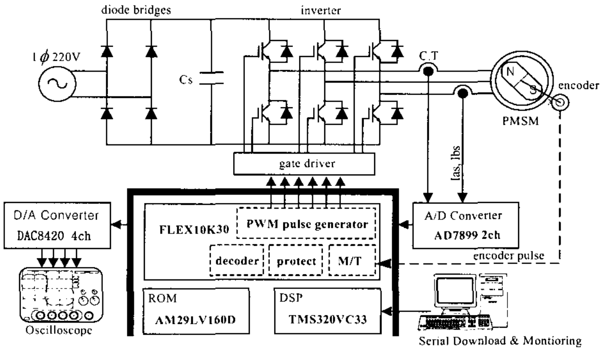

Fig. 6 Configuration of power circuit and drive system

The experimental result is obtained under the each error condition of $\Delta I_{as}=0.05[A]$, $\Delta I_{bs}=0.02[A]$, $K_a=1.2$ and $K_b=0.8$. Fig. 7 shows the steady state characteristics of the motor speed and the integral values of 6 segments before the compensation. The maximum speed ripple is about 0.5[rpm] and there exists an undesirable $1f_e$ and $2f_e$ of the speed ripples as shown in FFT analysis.

Fig. 8 shows the process of the compensation of current measurement errors. The ripple of Fig.8(c) is diminished by a method that looks for the compensating value in process.

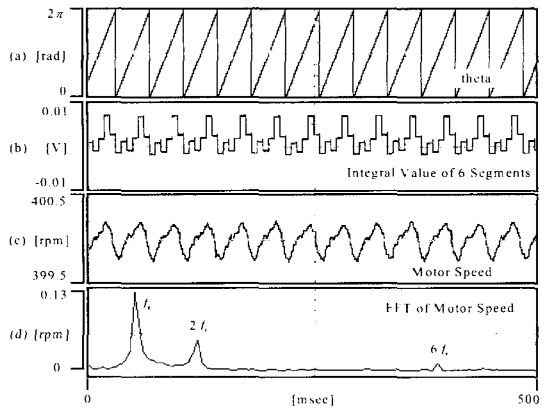

Fig. 7 Steady-state characteristics without compensation scheme

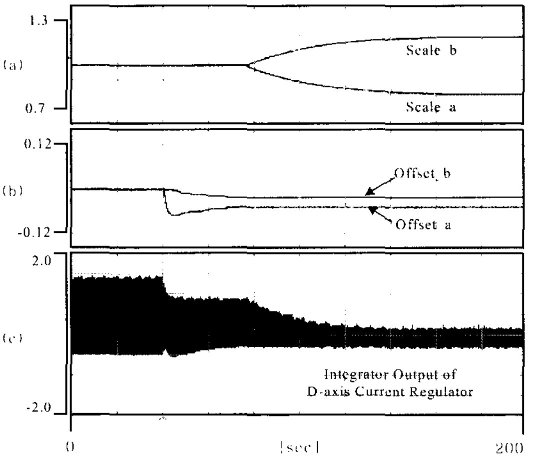

Fig. 8 Characteristics of compensating operation after flag-on

Fig. 9 shows the enlargement waveforms of Fig. 8 between 30[sec] and 80[sec]. After starting flag of compensation begins, the compensating algorithm operates well, and the steady state offset error is very small as shown in Fig. 9. But there is scaling error yet in Fig. 9.

After the compensation by the proposed method, speed ripples are eliminated almost completely to below 0.05[rpm] as shown in Fig. 10. $6f_e$ shows the influence of the dead time in Fig.10. The effect will not be mentioned in this paper. Several algorithms of the dead time have been published as mentioned before section.

Fig. 11 shows dynamic characteristics of current errors compensation in the transient state. In this experimental result, the proposed compensation algorithm has the attractive feature of transient state operation.

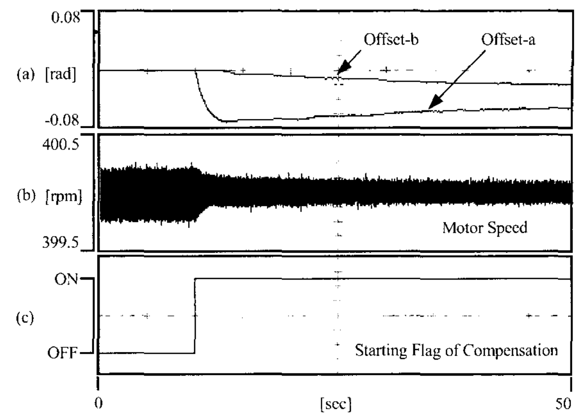

Fig. 9 Characteristics of compensating operation after flag-on (Enlargement waveforms of Fig.8 between 30[sec] and 80[sec])

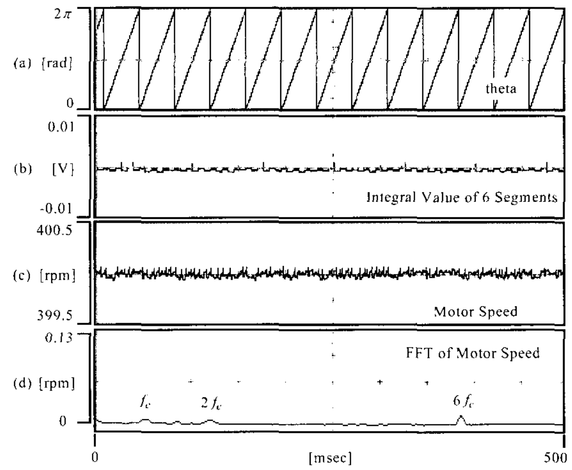

Fig. 10 Steady-state characteristics with proposed compensation scheme

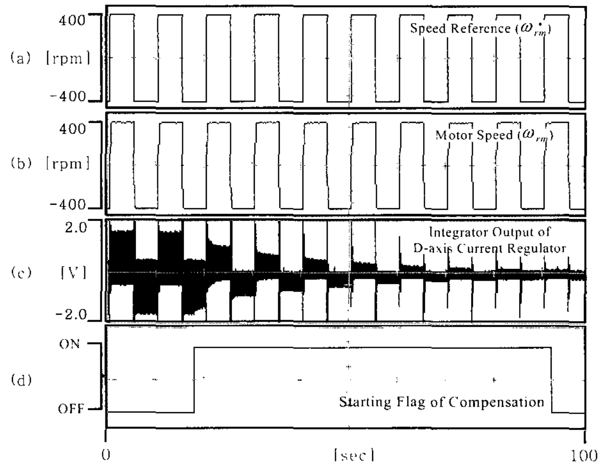

Fig. 11 Dynamic characteristics of compensation in the transient state. (±400[rpm] STEP)

6. Conclusion

In the digital AC motor drive system, the torque pulsation is caused by the offset and scaling error of the stator currents. Thus without the proper compensation algorithm, a higher performance vector control cannot be accomplished.

In this paper the new compensation algorithm was proposed. The main contribution of this paper introduces the signal of the integrator output of the d-axis current regulator to compensate the current errors. Usually the d-axis current command is zero or constant to acquire the maximum torque or unity power factor in the ac drive system, and the output of the d-axis current regulator is nearly zero or constant as well. Therefore, the proposed algorithm shows several features of the robustness in the variation of the machine variables, the application of the steady and transient state, the easy implementation, and requiring less computation time.

Through the simulation and experimentation, the feasibility and effectiveness of the proposed algorithm was verified.

References

[1] F. Colamartino, C. Marchand and A. Razek, "Torque ripple minimization in permanent magnet synchronous servo drive," IEEE Trans. Energy conversion, Vol. 14, No. 3, pp. 616-621, 1999.

[2] Seung-Ho Song, Jong-Woo Choi and Seung-Ki Sul, "Current Measurements in Digitally Controlled AC Drives," IEEE Industry Applications Magazine, Vol. 6, pp. 51-62, 2000.

[3] Texas Instruments, "Understanding Data Converters", Application report, 1995.

[4] Stefan Bruckl, "Feed-drive system with a permanent magnet linear motor for ultra precision machine tools," IEEE PEDS Conference, Vol. 2, pp.821-826, 1999.

[5] D. W. Chung, and S. K. Sul, "Analysis and Compensation of Current Measurement Error in Vector-Controlled AC Motor Drives,"IEEE Trans. On Industry Applications, Vol. 34, No. 2, pp. 340-345, 1998.

[6] B. H. Lam, S. K. Panda, J. X. Xu and K. W. Lim, "Torque ripple minimization in PM synchronous motor using iterative Learning control,"in proceedings of the 1999 Industrial Electronics Society Annual Conference of the IEEE, Vol. 3, pp. 1458-1463, 1999.

[7] Roberto Barro and Ping Hsu, "Torque Ripple Compensation of Induction Motors Under Field Oriented Control," IEEE APEC Conference, Vol. 1, pp. 527-533,1997.

[8] Weizhe Qian, S. K. Panda, J. X. Xu, "Reduction of Periodic Torque Ripple in PM Synchronous Motors using Learning Variable Structure Control," IEEE IECON Conf., Vvol. 2, pp. 1032-1037, 2002.

[9] Jong-Woo Choi, Sang-Sup Lee, Sang-Yeop Yu and Seok-Joo Jang, "Novel Periodic Torque Ripple Compensation Scheme in Vector Controlled AC Motor Drives," IEEE APEC Conference, Vol. 1, pp.81-85,1998.

[10] Ji-Hoon Jang, Seung-Ki Sul, and Yo-Chan Son, "Current Measurement Issues in Sensorless Control Algorithm using High Frequency Signal Injection Method," IEEE IAS Annual Meeting ,Vol. 2,pp. 1134 -1141, 2003.

[11] R. B. Sepe and J. H. Lang, "Inverter nonlinearities and discrete-time vector current control," IEEE Trans. Ind. Applicat., Vol. 30, pp.62-70, 1994.

[12] Jong-Woo Choi, Seung-Ki Sul, "New Dead Time Compensation Eliminating Zero Current Clamping in Voltage-Fed PWM Inverter,"IEEE Industry Applications Society Annual Meeting, pp.977-984, 1994.

[13] D. Antic, J. B. Klaassens and W. Deleroi, "Side Effects in Low-Speed AC Drives," IEEE Power Electronics Society Conference Record, pp.998-1002, 1994.

[14] G. Ferretti, G. Magnani and P. Rocco, "Modeling, identification, and compensation of pulsating torque in permanent magnet ac motors,"IEEE Trans. Ind. Elect., Vol. 45, No. 6, pp. 912-920.

[15] The Math Works. Inc., "SIMULINK Model Based and System Based Design",2002.

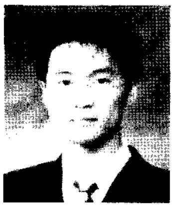

Han-Su Jung was born in the city of Geoje, Korea, in 1977. He received the B.S. degrees in electrical engineering from Gyeongsang National University, Jinju, Korea, in 2003. Since 2003, he has been with Department of Electrical Engineering, Pusan National University, where he is currently working toward the M.S. degree. His research interest is in the areas of electric machine drive, micro processor and power conversion.

Jang-Mok Kim was born in Busan, Korea, in August 1961. He received the B.S. degree from Pusan National University in 1988, and M.S. and Ph.D degree from Seoul National University, Korea, in 1991 and 1996, respectively, in Electrical Engineering. He is presently working toward the Ph.D. degree at Seoul National University. Previously, he joined the Korea Electrical Power Research Institute as senior research engineer from 1997 to 2000. Since 2001, he has been a faculty member in the division of Electrical and Electronics Engineering, Pusan National University, serving as a assistant professor. And he is a research member of the research institute of Computer Information and Communication in Pusan national University. His present interests are in power electronic control of elcecrtic machine, and power quality.

Cheul-U Kim (S'85–M'87) received the B.S. degree in Electrical Engineering from Pusan National University, Busan, Korea in 1969, the M.S. degree from the University of Electro-Communications, Japan, in 1974, and the Ph.D. degree from Chung-Ang University, Korea, in 1986. Since 1975, he has been a professor at Pusan National University, Busan, Korea. His research activities are in the area of power electronics and motor control, including cyclo-converter designs, drive systems, and high efficiency switch mode power supplies. His current research interests include the design of high efficient sustain driver for ac plasma display panel driving. Dr. Kim is a member of the Korea Institute of Electrical Engineering, Korea Institute of Power Electronics, Korea Institute of Illuminating and Electrical installation Engineers, and Japan Institute of Electrical Engineers.

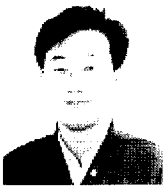

Cheol, Choi was born in 1963. He received the B.S degree in Electrical Engineering from Chung-Ang University, Seoul, Korea, in 1987, and the M.S. degree in Electronics Engineering from Kyeongnam University, Masan, Korea, in 1994, and the M.S. degree in Electrical Engineering from Pusan University, Pusan, Korea, in 1998. He received Ph. D in Electrical Engineering from Pusan University, Pusan, Korea, in 2005. He have worked at LGIS Parking Facilities Division from 1986 to 1999. He is now working at OTIS.LG Motor Division Servo Team from 1999. He is interested in power electronics and its application.

Tae-Uk Jung was born in Masan, Korea on May 16, 1970. He received the B.S., M.S. and Ph.D. degrees in electrical engineering from Busan National University, Busan, Korea, in 1993, 1995 and 1999, respectively. Since 1996, he has been with Laboratory of LG Electronics, Korea, where he is currently a Chief Research Engineer and is engaged in research on high efficiency motor design and application. Dr. Jung is interested in high efficient motor design and their control and application. He is a member of the Institute of Electrical Engineers of Korea (KIEE).